

Initial study and design on ignition ellipraum

KE LAN, DONGXIAN LAI, YIQING ZHAO, AND XIN LI

Institute of Applied Physics and Computational Mathematics, Beijing, People's Republic of China

(RECEIVED 1 November 2011; ACCEPTED 17 November 2011)

Abstract

An initial study and design on ignition elliptical hohlraum (ellipraum) is given by using the expended plasma-filling model with criterions. As a result, in an ellipraum with a smaller ratio of major-to-minor axis (a/b), the radius ratio of ellipraum-to-capsule (b/R_c) should be larger (hence more sphere-like) to meet the criterions of plasma-filling and laser deposition, meanwhile the required laser energy and peak power are lower and the coupling between different modes is weaker. To produce a 300 eV radiation pulse to ignite a capsule of 1 mm radius, an ellipraum of $a/b = 1.6$ and $b/R_c = 2.8$ is superior to a cylinraum with a length-to-diameter ratio of 1.81 and a cylinraum-to-capsule radius ratio of 2.54 in saving more than 10% laser energy and reducing 50% coupling between different modes.

Keywords: Elliptical hohlraum; Inertial fusion; Plasma filling

1. INTRODUCTION

Hohlraum plays a key role in indirect drive inertial fusion (Haan *et al.*, 1995, 2011; Atzeni & Meyer-ter-Vehn, 2004; Lindl *et al.*, 2004), which converts incident laser beam into X-rays to uniformly drive a capsule placed inside the hohlraum to ignite. Because many factors that greatly influence the ignition are strongly related to the hohlraum geometry, such as the coupling efficiency from hohlraum to capsule, the X-ray emission, capsule radiation uniformity, and laser plasma interactions, so the design of hohlraum is very important (Callahan, 2006, 2008; Li, 2010; Lan, 2010; Rosen, 2011). The traditional hohlraum is a cylinder (hereafter called “cylinraum”), now being used for the national ignition campaign (Haan *et al.*, 2011). However, in order to have a more efficient hohlraum, researchers have also been making efforts in exploiting hohlraums with different shapes. Elliptical hohlraum (hereafter called “ellipraum”) was first proposed in 1991 (Caruso, 1991), but until recent years, it began to arouse much interests worldwide. Up to now, there are many simulation design and experiments on rugby-like or ellipraums for the OMEGA and the LMJ laser facilities (Amendt, 2007, 2008; Vandenboomgaerde, 2007; Casner, 2009; Robey, 2010; Philippe, 2010). These shapes of hohlraum have the possible advantages over cylinraum in enhancing X-ray drive and reducing mode coupling

for symmetry control, and this has already been demonstrated (Vandenboomgaerde, 2007; Robey, 2010). Presently, the main strategy to design a rugby-like or ellipraum was given by Amendt *et al.* (2008).

In this work, we will present our initial study and design on ignition ellipraum by using the extended plasma-filling model with criterions of plasma-filling and laser deposition (Lan, 2010), and give an initial design of ellipraum size and pertinent laser power to produce a typical 300 eV ignition radiation (Callahan, 2008). In addition, we will compare the mode coupling efficiencies in ellipraum and cylinraum. For a hohlraum with given shape, there are three ratios to describe the hohlraum geometry, which are the ratio of hohlraum semi length-to-radius, the radius ratio of hohlraum-to-capsule, and the radius ratio of laser entrance hole (LEH) to capsule, respectively, denoted as ξ_H , ξ_C , and ξ_L hereafter. Usually, the capsule radius is given by the implosion design and the LEH sizes is decided by the laser beam conditions, so only ξ_H and ξ_C are left to design. Here, we want to make clear that there are two points in our design strategy different from that of Amendt *et al.* (2008). First, Amendt *et al.* (2008) keep the same ξ_C of rugby-like hohlraum as that of the compared cylinraum, then used the calculus of variations to assess the minimal surface area for a given enclosed hohlraum volume in order to decide the detail hohlraum shape; while in our design, we directly used ellipraum, which schematic is show in Figure 1. Second, Amendt *et al.* (2008) adjust ξ_H (and laser cone pointings) of the rugby-like hohlraum with chosen shape to

Address correspondence and reprint requests to: Ke Lan, Institute of Applied Physics and Computational Mathematics, P.O. Box 8009-14 Beijing, 100088, People's Republic of China. E-mail: ke_lan68@yahoo.com

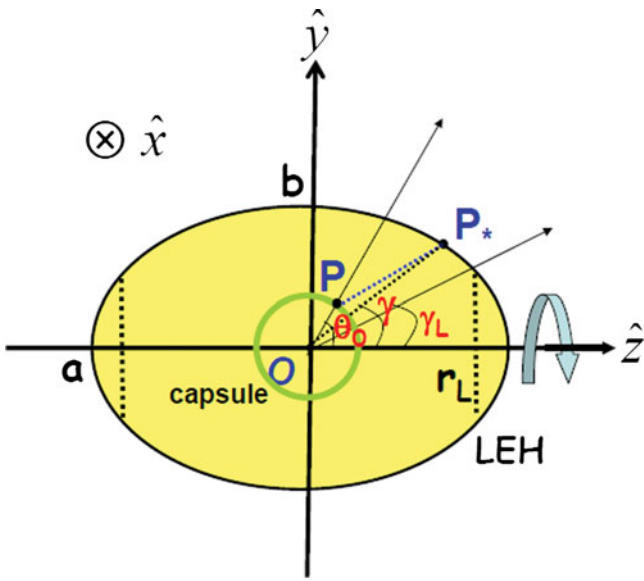


Fig. 1. (Color online) Geometry for ellipraum and capsule. Here, **O** is the center, **P** is point on capsule and **P*** is a point on ellipraum surface.

achieve optimal implosion core symmetry; while in our design, we obtain ξ_C from the extended plasma-filling model with criterions to meet the requirements of plasma-filling and laser deposition at different ξ_H , and ξ_H will be decided by a two-dimensional (2D) simulation. Because the optimal ξ_H is relevant to the tolerable LEH size and the laser beam arrangement, so a detail 2D simulation is needed to optimize the ellipraum size together with the laser pointing position, and the relative beam powers after balancing all factors. We will present our 2D simulation in a forthcoming paper, and will only focus on the initial design in this work. As a result, ξ_C of ellipraum from our design is higher than that of the rugby-like hohlraum designed by Amendt *et al.* (2008), and also the coupling from hohlraum to capsule in our ellipraum is lower than their rugby. Notice that the intents are different in the two designs. Amendt *et al.* (2008) intend to drive high yield with low-convergence capsules, so they design a rugby-like hohlraum with a smaller volume and a smaller ξ_C to get a higher coupling efficiency from hohlraum to capsule than our design, and they did successfully obtain a very high X-ray enhancement and very high neutron yield with the rugby-like hohlraum compared with the cylindraum, while they also observed a significantly high simulated Brillouin scattering backscatter that affect the implosion symmetry (Robey, 2010). Our intent in this work is to design an ellipraum for ignition. Hence, in addition to the enhancement of X-ray radiation, the plasma-filling is an important issue to concern in our work.

This work is arranged as follows. In Section 2, we will apply the extended plasma-filling mode in ellipraum and give criterions of plasma-filling and laser deposition. In Section 3, we will present our method to give an initial design of hohlraum size and pertinent laser power to produce a

required radiation inside the hohlraum, and then give an initial design of ellipraum to produce a 300 eV ignition radiation. In Section 4, we will compare the mode coupling efficiencies in ellipraum with that in cylindraum. Finally, we summarize in Section 5.

2. EXTENDED PLAMAS-FILLING MODEL FOR ELLIPRAUM

In our previous work (Lan *et al.*, 2010), we extended the plasma-filling model (Dewald *et al.*, 2005; McDonald *et al.*, 2006; Schneider *et al.*, 2006) to a case when a cylindraum is driven by a shaped laser pulse with high contrast (>1) between different steps, which is a typical drive for ignition goal. In the extended model, we assume that the differences of radiation temperature T_r between steps are large and calculate the ablated mass of the wall in each step independently. The ablation in each step increases the wall albedo and contributes to the sum of the ablated mass, and therefore eventually influences the plasma-filling time in hohlraum. In this part, we apply this extended plasma-filling model to an ellipraum.

For an ellipraum considered in our study, it rotates along its major axis and the LEH are opened at both ends of ellipraum along the major axis, in order to keep the radiation uniformity of capsule inside. The schematic of an ellipraum is shown in Figure 1. We use a to denote the major axis of an ellipraum, b is the minor axis, R_L is the radius of LEH, and γ_L is the angle of LEH to the rotating axis z . Defining $e = \sqrt{|a^2 - b^2/a^2|}$ and $t = a\sqrt{1 - r_L^2/b^2}$, then we have $\gamma_L = \arccos\left(t/\sqrt{r_L^2 + t^2}\right)$. Thus, the wall area A_W and volume V_H can be, respectively, expressed as:

$$A_W = 2\pi ab \left[\cos \gamma_L \times \sqrt{1 - e^2 \cos^2 \gamma_L} + \frac{1}{e} \times \arcsin (e \cos \gamma_L) \right], \tag{1}$$

$$V_H = 2\pi ab^2 \left(\cos \gamma_L - \frac{\cos^3 \gamma_L}{3} \right). \tag{2}$$

We use A_L to denote the area of LEH and A_C to denote the area of capsule. Under the j th step of a laser pulse, the geometrical factor f_j of hohlraum with a capsule inside is (Sigel *et al.*, 1988):

$$f_j = 1 + \frac{(1 - \alpha_{C,j})A_C + A_L}{(1 - \tilde{\alpha}_{W,j})A_W}. \tag{3}$$

Here, $\alpha_{C,j}$ is the albedo of capsule and $\tilde{\alpha}_{W,j}$ is an effective albedo of the wall under the j th step. Thus, the hohlraum power balance (Lindl, 1995) under the j th step pulse

$$\eta P_j = [(1 - \alpha_{W,j})A_W + (1 - \alpha_{C,j})A_C + A_L] \sigma T_{r,j}^4,$$

can be written as:

$$\eta P_j = (1 - \alpha_{w,j}) f_j A_w \sigma T_{r,j}^4. \quad (4)$$

Here, P_j is laser power at the j th step, and σ is the Stefan-Boltzmann constant. Usually, the wall albedo at time τ under a radiation temperature of T_r can be expressed as (Lindl, 1995):

$$\alpha_w = 1 - H / (T_r^\gamma \tau^\beta), \quad (5)$$

where H , γ , and β are fitting parameters. Therefore, we can express $T_{r,j}$ as (Lindl, 1995):

$$T_{r,j} = D P_j^E \tau_j^F. \quad (6)$$

Here, the coefficients D , E , and F can be obtained by taking Eq. (5) into Eq. (4), and they are related to the laser power at every step.

Summing the radiation ablated mass under all laser pulse steps; we get the material density inside hohlraum (Schneider *et al.*, 2006):

$$\rho = \frac{A_{abl}}{V_H} \times \sum_j m_j. \quad (7)$$

Here, m_j is the area mass ablated in the j th step of radiation, A_{abl} is an effective ablated wall area. Considering the hydrodynamic losses and coronal radiative losses from LEH, we take $A_{abl} = A_w - A_{LEH}$, here A_{LEH} is the area of LEH. Then, the ion density n_i is:

$$n_i = \frac{536}{A} \times \lambda_L^2 \times \frac{A_{abl}}{V_H} \times \sum_j m_j. \quad (8)$$

Here, n_i is in units of the critical density, A is the atomic number of wall material, λ_L (in μm) is the wavelength of driven laser, A_{abl} is in cm^2 , V_H is in cm^3 , and m_j is in g/cm^2 .

Furthermore, as in the plasma-filling model (Schneider, 2006), considering the power balance of the laser hot channel and the pressure balance between the laser channel and surrounding plasmas, we can finally obtain the average electron density n_e in laser hot channel at filling time (Lan *et al.*, 2010).

Because n_e depends on laser pulse, wall material, and hohlraum size, so the plasma-filling model can be used in the initial design of a hohlraum target. More than that, the plasma-filling model can be actually applied to the initial design of an ignition hohlraum, although the latter usually uses low- Z gases fill to suppress hohlraum high- Z plasma expansion, while the former normally refers to the vacuum hohlraums filled with high- Z plasmas due to laser heating. The reason is that, from our 2D simulations, the low- Z gases fill does play an important role in suppressing hohlraum high- Z plasma expansion and helping to improve the

radiation uniformity on capsule during the pre-pulses of driving laser, but its role can be almost neglected when very hot and massive hohlraum high- Z plasmas is ablated during the main pulse. In other words, the hohlraum filling during the main pulse of laser heating is also mainly caused by the high- Z wall plasmas for an ignition target. Therefore, an initial design of ignition hohlraum can be obtained from the plasma-filling model.

Certainly, criterion is needed to design a suitable hohlraum for ignition besides the requirement on hohlraum geometrical factors from capsule radiation uniformity. As known (Schneider *et al.*, 2006), when the plasma filling becomes serious, the laser absorption region shifts far from the hohlraum wall and the hydrodynamic loss and the thin coronal radiative loss from LEH increase rapidly. Usually, $n_e = 0.1$ is used as a threshold that prevents the laser from propagating into the hohlraum due to absorption. On the other hand, the laser is required to deposit near the wall surface for an ignition target in order to get X-ray emission near hohlraum wall. Therefore, we define two semi-empirical criterions for ignition hohlraum. One criterion is $n_e = 0.1$, and another one is $n_{IB} = 1$. Here, n_{IB} can be defined either as $(R / (\sqrt{2} \sin \delta)) / (\lambda_{IB})$ or $(\sqrt{2} R_{LEH} / \sin \delta) / (\lambda_{IB})$, in which λ_{IB} is the inverse bremsstrahlung absorption length (Dawson *et al.*, 1969) and δ is an effective incident angle of laser to hohlraum axis. According to our experience, we usually take $\delta = 50^\circ$ for ignition design. Under different criterion, it may give a different size of hohlraum. We choose the largest hohlraum as our initial design after considering all the criterions. Hereafter, the extended plasma-filling model with criterions is shortened as EPFC.

3. INITIAL DESIGN OF ELLIPRAUM UNDER 300 EV IGNITION RADIATION

The above EPFC, together with one-dimensional (1D) simulation, can be used to give an initial design of hohlraum size and pertinent laser power to produce a required radiation inside the hohlraum. In this part, we first present our initial design method, and then use it to design an ellipraum and pertinent laser power to produce a 300 eV radiation pulse for a given capsule.

As discussed in Section 1, R_C is given by implosion design, ξ_L is usually decided by the laser beam conditions, and ξ_H will be chosen by 2D simulation after taking the laser beam conditions into consideration. Hence, what we need to give from the initial design is ξ_C at different ξ_H . In addition, we need some iteration in the initial design so as to get P_j , the laser power at the j th step. Our initial design method has five steps:

- (1) As the first step, we have to assume a primary value of ξ_C at a given ξ_H , such as taking the values from traditional cylinder in which the radiation uniformity has already been taken into consideration. Because

R_C is given, we therefore have the primary values of a , b , R_L .

- (2) Then we have the time-dependent wall albedo and capsule albedo under the required radiation pulse from 1D simulation.
- (3) After that, we obtain the primary profile of laser power by putting the albedo of wall, the albedo of capsule, and the primary ellipraum size into the hohlraum power balance. Thus, all coefficients needed in Eqs. (5) and (6) can be obtained.
- (4) Furthermore, we obtain the first design of ellipraum size by using EPFC.
- (5) If the first size is smaller than the primary size, then we take the primary size and the primary laser power as the initial design result. Otherwise, we modify the laser power profile by putting the first size into the power balance and recalculate all coefficients, and then we obtain the second size from EPFC. We iterate this process until the profile of laser power is convergent. Finally, the convergent laser power and relevant hohlraum size are the initial design result.

As an example, now we give an initial design of ellipraum and pertinent laser power to produce the 300 eV radiation pulse in the 2010 ignition target design on the NIF (Callahan et al., 2008). This radiation pulse has four steps, as shown in Figure 2. The coupling efficiency from laser to X-ray is taken as 75%. To compare with the design given in Callahan et al. (2008), we also take $R_c = 1$ mm and $\xi_L = 1.27$. About ξ_H , usually it is taken from 1.7 to 1.81 for inertial fusion study (Lindl, 1995; Cavailler, 2005; Callahan, 2008; Haan, 2011). Here, we take $\xi_H = a/b$ as 1.4, 1.6, 1.8, and 2 for ellipraum. In addition, we also consider one model for cylindraum of $\xi_H = 0.5L/R = 1.81$, same as in Callahan (2008), just for comparison.

First, we calculate the albedo of U under the 300 eV radiation pulse by using our 1D multi-groups radiation transfer code, radiation hydrodynamic code of multi-groups

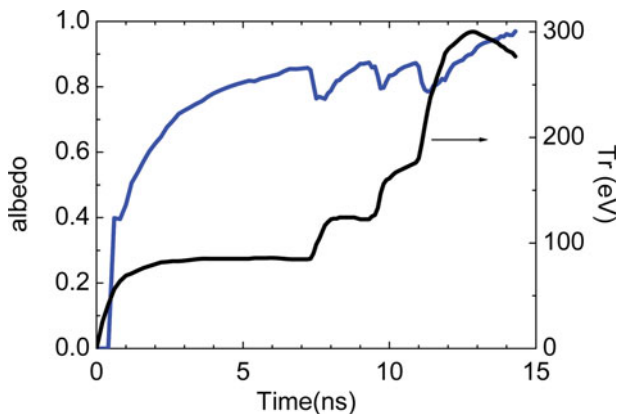


Fig. 2. (Color online) Albedo (blue line) of U wall from RDMG code under 300 eV radiation pulse (black line) given in Callahan (2008).

(RDMG) (Feng et al., 1999), as shown in Figure 2. Then, following the initial design method given above, we finally obtain the contour lines of $T_r = 300$ eV, $n_e = 0.1$, and $n_{IB} = 1$ in the plane of laser energy E_L and hohlraum semi-length at a given ξ_H for ellipraum or cylindraum. The contour line of $T_r = 300$ eV may have different intersections with contour lines of $n_e = 0.1$ and $n_{IB} = 1$, resulting in two sizes of hohlraum and two laser energies. We take the larger size with higher laser energy as our initial design. As shown in Figure 3, are initial design results for the five kinds of hohlraums.

For cylindraum, our initial design gives a result of 9.1 mm length with 0.93 MJ laser energy, which is close to the design given in Callahan et al. (2008).

For ellipraum, the intersections give: (1) $a = 4$ mm and $E_L = 0.8$ MJ at $\xi_H = 1.4$; (2) $a = 4.48$ mm and $E_L = 0.83$ MJ at $\xi_H = 1.6$; (3) $a = 4.95$ mm and $E_L = 0.85$ MJ at $\xi_H = 1.8$; and (4) $a = 5.4$ mm and $E_L = 0.88$ MJ at $a/b = 2$. Notice that the laser energy required for the four ellipraums is obviously smaller as compared with the cylindraum. From a , ξ_H , and R_c , we can obtain ξ_C : (1) $\xi_C = 2.86$ at $\xi_H = 1.4$; (2) $\xi_C = 2.8$ at $\xi_H = 1.6$; (3) $\xi_C = 2.75$ at $\xi_H = 1.8$, and (4) $\xi_C = 2.7$ at $\xi_H = 2$. As a result, the initial design gives a lower E_L and a larger ξ_C at a shorter ξ_H , which certainly benefits to save laser energy and improve capsule radiation uniformity.

From Eq. (7), the filling density inside hohlraum is related to the ratio of wall area to hohlraum volume. Table 1 lists the area and volume ratios of ellipraum-to-cylindraum for above models, which helps us to understand the advantage of ellipraum in saving laser energy while meeting the plasma-filling requirement at the same time. From Table 1, both ellipraum volume and area are smaller as compared

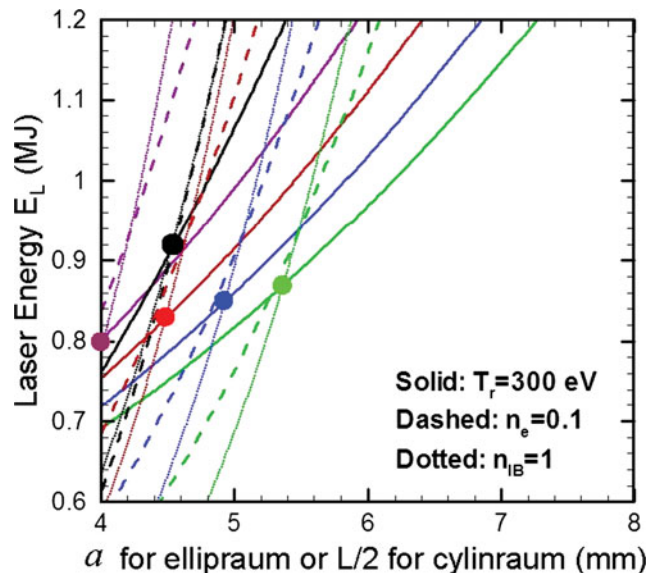


Fig. 3. (Color online) Initial design of laser energy and hohlraum size to produce a 300 eV ignition radiation in ellipraums of $\xi_H = 1.4$ (violet), 1.6 (red), 1.8 (blue), and 2.0 (green) and in a cylindraum of $\xi_H = 1.81$ (black).

Table 1. Volume and area ratios of ellipraum-to-cylindraum. Here, the compared cylindraum is at $\xi_H = 1.81$ and $\xi_C = 2.54$. The values of ξ_H and ξ_C given in the table are for ellipraum. Here, the subscripts “ellip” and “cylin” refer respectively to ellipraum and cylindraum. In addition, A_{abl} is also listed for comparison.

$\xi_H \times \xi_C$	1.4 × 2.86	1.6 × 2.8	1.8 × 2.75	2 × 2.7
V_{ellip}/V_{cylin}	0.73	0.786	0.839	0.883
$A_{W,ellip}/A_{W,cylin}$	0.704	0.761	0.816	0.865
$A_{abl,ellip}/A_{abl,cylin}$	0.686	0.747	0.805	0.857
$A_{W,ellip}/A_{W,cylin}$ V_{ellip}/V_{cylin}	0.964	0.968	0.972	0.98
$A_{abl,ellip}/A_{abl,cylin}$ V_{ellip}/V_{cylin}	0.94	0.95	0.96	0.97

with the cylindraum, but the ellipraum area is much smaller. It is easy to understand when a sphere is associated. As a result, either $(A_{W,ellip}/A_{W,cylin})/(V_{ellip}/V_{cylin})$ or $(A_{abl,ellip}/A_{abl,cylin}/V_{ellip})/(V_{cylin})$ are smaller than 1, but very near to 1 to meet the criterions. They do not exactly equal to 1 because the coefficients in Eq. (6) are also related to the wall area.

In Figure 4, we give the pertinent laser power to produce the 300 eV radiation pulse in the ellipraum of $a/b = 1.6$ and $b/R_c = 2.8$. The result for the cylindraum is also presented for comparison. As shown, the required peak power is 300 TW for the ellipraum, which is about 10% lower than what required for the cylindraum.

4. THE COUPLING BETWEEN DIFFERENT MODES IN AN ELLIPRAUM

As we know, it is a key requirement in ignition research to control capsule implosion symmetry (Lindl, 2004; Haan, 2011). For Legendre asymmetry modes, P_2 and P_4 are

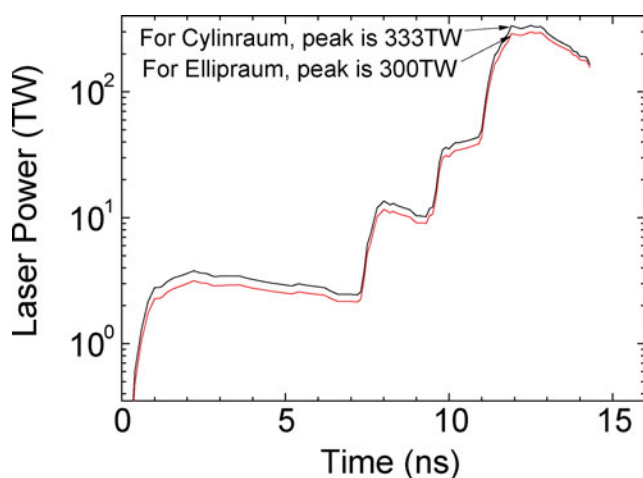


Fig. 4. (Color online) Laser powers to produce the 300 eV ignition radiation in an ellipraum of $\xi_H = 1.6$ and in a cylindraum of $\xi_H = 1.81$.

main issues in hohlraums of $\xi_C < 4$. Normally, P_4 is controlled by laser ring separation and P_2 is controlled with the inner/outer cone ratio (Lindl, 2004). However, there is coupling between modes for capsule in non-spherical hohlraums (Suter, 1985; Lindl, 2004), because different points on the capsule see different solid angles of the hohlraum wall and therefore have different smoothing factors. It means that P_2 and all higher even modes appear at the capsule even if only a pure P_2 is applied to the hohlraum. Nevertheless, the coupling between modes is relevant to hohlraum shape and it is somewhat easier to control in a hohlraum with weaker coupling. In this part, we compare the coupling between modes in an ellipraum with that in a cylindraum.

As in Caruso and Strangio (1991), we consider a capsule that is illuminated by the radiation emitted from an optically thin plasma layer at the ellipraum surface. The geometry of ellipraum and capsule is shown in Figure 1, and the geometry relevant for the definition of position between point \mathbf{P} on capsule and point \mathbf{P}^* on ellipraum surface is shown in Figure 5. We use $I(\mathbf{P}^*)$ to denote the emitted power density from \mathbf{P}^* , then the total power density flux F at \mathbf{P} is:

$$F(\mathbf{P}) = \int_0^\pi \cos \theta \sin \theta \int_0^{2\pi} I(\mathbf{P}^*) d\phi. \tag{9}$$

Both ellipraum and radiation source distribution are cylindrical symmetry in our consideration. Then $I(\mathbf{P}^*)$ can be represented in terms of Legendre polynomials P_n with argument of $\cos \gamma$, where γ is the angle of \mathbf{OP}^* with the symmetry axis, as in Figure 1:

$$I(\mathbf{P}^*) = \sum_{n=0}^{\infty} c_n P_n(\cos \gamma). \tag{10}$$

On the other hand, the radiation on capsule can also be

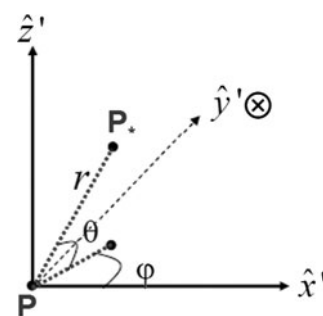


Fig. 5. Geometry relevant for the definition of the position between point \mathbf{P} on capsule and point \mathbf{P}^* on ellipraum surface. Here, z' is in the direction of \mathbf{OP} , both x' and y' are tangential directions, and y' is defined to point into paper.

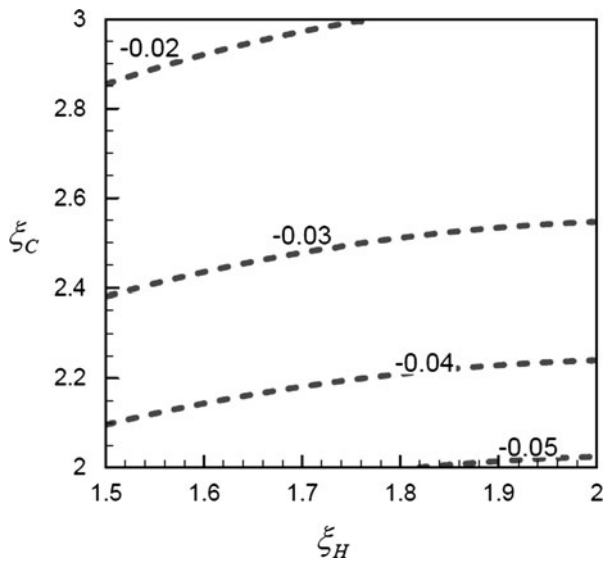


Fig. 6. Contour lines of (P_4) on capsule when (P_2) is applied to cylindraum, in the plane of ξ_H and ξ_C .

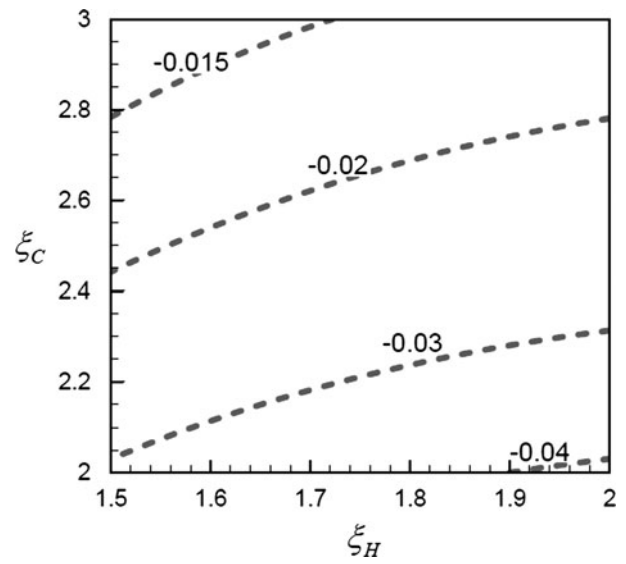


Fig. 8. Contour lines of (P_4) on capsule when (P_2) is applied to ellipraum, in the plane of ξ_H and ξ_C .

represented in terms of P_n but with argument of $\cos \theta_0$:

$$F(\mathbf{P}) = \sum_{n=0}^{\infty} a_n P_n(\cos \theta_0). \tag{11}$$

Here, we call $a_m(P_n)$ as the coupling coefficient between the modes m and n when a pure P_n ($c_n = 1$) is applied to the hohlraum.

In Figures 6 and 7, it gives $a_4(P_2)$ and $a_2(P_4)$ for cylindraum in the plane of ξ_H and ξ_C . In Figures 8 and 9, it gives $a_4(P_2)$ and $a_2(P_4)$ for ellipraum in the plane of ξ_H and ξ_C . Usually, the cylindraum designed for ignition study has ratio

values of about $\xi_H = 1.6-1.8$ and $\xi_C = 2.5$. Here we choose the ellipraum of $\xi_H = 1.6$ and $\xi_C = 2.8$ for comparison. Then, as shown, $a_4(P_2) = -0.03$ and $a_2(P_4) = -0.07$ for the cylindraum, while $a_4(P_2) \approx -0.015$ and $a_2(P_4) \approx -0.035$ for the ellipraum. Hence, the mode coupling in the ellipraum is about half of that in the cylindraum. In fact, the mode coupling is weaker in a more sphere-like hohlraum, which benefits to control the different modes separately.

5. SUMMARY

We have applied EPFC to give an initial design on ignition elliptical hohlraum and pertinent laser pulse to generate a

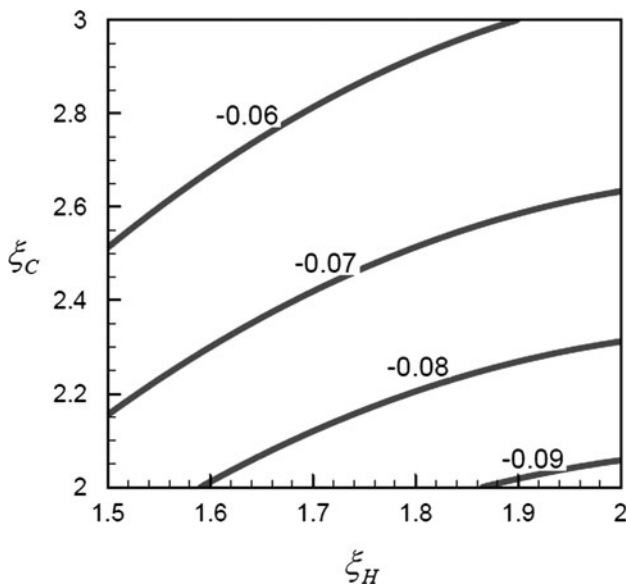


Fig. 7. Contour lines of (P_2) on capsule when (P_4) is applied to cylindraum, in the plane of ξ_H and ξ_C .

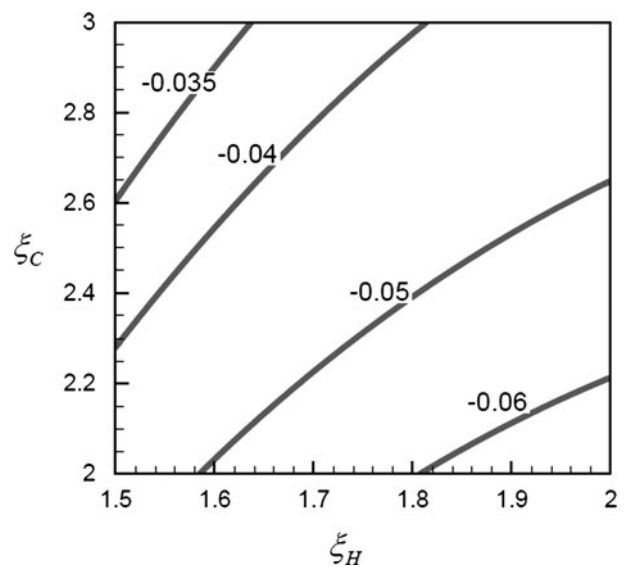


Fig. 9. Contour lines of (P_2) on capsule when (P_4) is applied to ellipraum, in the plane of ξ_H and ξ_C .

required radiation pulse. We have also compared the mode coupling between ellipraum and cylinraum. As a result, in an ellipraum with a smaller ξ_H , the value of ξ_C should be larger in order to satisfy the criterions of plasma-filling, meanwhile the required laser energy and peak power are lower and also the coupling between different modes is weaker. In addition, a large ξ_C has the benefit in capsule radiation uniformity. To produce a 300 eV radiation pulse inside hohlraum to ignite a capsule of 1 mm radius, an ellipraum of $\xi_H = 1.6$ and $\xi_C = 2.8$ is superior to a cylinraum of $\xi_H = 1.81$ and $\xi_C = 2.54$ in saving more than 10% laser energy and reducing 50% coupling between different modes, here the radius of laser entrance hole is taken as 1.27 mm.

However, the optimal ξ_H and ξ_C for ellipraum are also relevant to the tolerable R_L and the laser beam arrangement. The transfer distance of laser beam inside the ellipraum of $\xi_H = 1.6$ and $\xi_C = 2.8$ is shorter than inside the cylinraum of $\xi_H = 1.81$ and $\xi_C = 2.54$ when laser incident angle is larger than 50° , but longer when the angle is smaller than 50° . Therefore, a detail 2D simulation is needed to determine the optimum ellipraum size, the pointing position and the relative beam powers after balancing all factors.

ACKNOWLEDGMENTS

The authors wish to acknowledge the beneficial discussions with Prof. Min Yu and Prof. Yongkun Ding.

REFERENCES

- AMENDT, P., CERJAN, C., HAMZA, A., HINKEL, D.E., MILOVICH, J.L. & ROBEY, H.F. (2007). Assessing the prospects for achieving double-shell ignition on the National Ignition Facility using vaccum hohlraums. *Phys. Plasmas* **14**, 056312.
- AMENDT, P., CERJAN, C., HINKEL, D.E., MILOVICH, J.L., PARK, H.-S. & ROBEY, H.F. (2008). Rugby-like hohlraum experimental designs for demonstrating X-ray drive enhancement. *Phys. Plasmas* **15**, 012702.
- ATZENI, S. & MEYER-TER-VEHN, J. (2004). *The Physics of Inertial Fusion*. Oxford: Oxford Science Press.
- CALLAHAN, D.A., AMENDT, P., DEWALD, E.L., HAAN, S.W., HINKEL, D.E., IZURNI, N., JONES, O.S., LANDEN, O.L., LINDL, J.D., POLLAINÉ, S.M., SUTER, L.J., TABAK, M. & TURNER, R.E. (2006). Using laser entrance hole shields to increase coupling efficiency in indirect drive ignition targets for the National Ignition Facility. *Phys. Plasmas* **13**, 056307.
- CALLAHAN, D.A., HINKEL, D.E., BERGER, R.L., DIVOL, L., DIXIT, S.N., EDWARDS, M.J., HAAN, S.W., JONES, O.S., LINDL, J.D., MEEZAN, N.B., MICHEL, P.A., POLLAINÉ, S.M., SUTER, L.J. & TOWN, R.P.J. (2008). Optimization of the NIF ignition point design hohlraum. *J. Phys. Confer. Ser.* **112**, 022021.
- CARUSO, A. & STRANGIO, C. (1991). The quality of the illumination for a spherical capsule enclosed in a radiating cavity. *Jpn. J. Appl. Phys.* **30**, 1095.
- CASNER, A., GALMICHE, D., HUSER, G., JADAUD, J.-P., LIBERATORE, S. & VANDENBOOMGAERDE, M. (2009). Indirect drive ablative Rayleigh–Taylor experiments with rugby hohlraums on OMEGA. *Phys. Plasmas* **16**, 092701.
- CAVAILLER, C. (2005). Inertial fusion with the LMJ. *Plasma Phys. Control. Fusion* **47**, B389–B403.
- DAWSON, J., KAW, P. & GREEN, B. (1969). Optical absorption and expansion of laser-produced plasmas. *Phys. Fluids* **12**, 875.
- DEWALD, E.L., SUTER, L.J., LANDEN, O.L., HOLDER, J.P., SCHEIN, J., LEE, F.D., CAMPBELL, K.M., WEBER, F.A., PELLINEN, D.G., SCHNEIDER, M.B., CELESTE, J.R., MCDONALD, J.W., FOSTER, J.M., NIEMANN, C.J., MACKINNON, A., GLENZER, S.H., YOUNG, B.K., HAYNAM, C.A., SHAW, M.J., TURNER, R.E., FROULA, D., KAUFFMAN, R.L., THOMAS, B.R., ATHERTON, L.J., BONANNO, R.E., DIXIT, S.N., EDER, D.C., HOLTMEIER, G., KALANTAR, D.H., KONIGES, A.E., MACGOWAN, B.J., MANES, K.R., MUNRO, D.H., MURRAY, J.R., PARHAM, T.G., PISTON, K., VAN WONTERGHEM, B.M., WALLACE, R.J., WEGNER, P.J., WHITMAN, P.K., HAMMEL, B.A. & MOSES, E.I. (2005). Radiation-driven hydrodynamics of high-Z hohlraums on the national ignition facility. doi: 10.1103/PhysRevLett.95.215004.
- FENG, T.G., LAI, D.X. & XU, Y. (1999). An artificial-scattering iteration method for calculating multi-group radiation transfer problem. *Chinese J. Comput. Phys.* **16**, 199–205.
- HAAN, S.W., POLLAINÉ, S.M., LINDL, J.D., SUTER, L.J., BERGER, R.L., POWERS, L.V., ALLEY, W.E., AMENDT, P.A., FUTTERMAN, J.A., LEVEDAHL, W.K., ROSEN, M.D., ROWLEY, D.P., SACKS, R.A., SHESTAKOV, A.I., STROBEL, G.L., TABAK, M., WEBER, S.V. & ZIMMERMAN, G.B. (1995). Design and modelling of ignition targets for the National Ignition Facility. *Phys. Plasmas* **2**, 1635.
- HAAN, S.W., LINDL, J.D., CALLAHAN, D.A., CLARK, D.S., SALMONSON, J.D., HAMMEL, B.A., ATHERTON, L.J., COOK, R.C., EDWARDS, M.J., GLENZER, S., HAMZA, A.V., HATCHETT, S.P., HERRMANN, M.C., HINKEL, D.E., HO, D.D., HUANG, H., JONES, O.S., KLINE, J., KYRALA, G., LANDEN, O.L., MACGOWAN, B.J., MARINAK, M.M., MEYERHOFER, D.D., MILOVICH, J.L., MORENO, K.A., MOSES, E.I., MUNRO, D.H., NIKROO, A., OLSON, R.E., PETERSON, K., POLLAINÉ, S.M., RALPH, J.E., ROBEY, H.F., SPEARS, B.K., SPRINGER, P.T., THOMAS, C.A., TOWN, R.P., VESEY, R., WEBER, S.V., WILKENS, H.L. & WILSON, D.C. (2011). Point design targets, specifications, and requirements for the 2010 ignition campaign on the National Ignition Facility. *Phys. Plasmas* **18**, 051001.
- LAN, K., GU, P., REN, G., LI, X., WU, C., HUO, W., LAI, D. & HE, X. (2010). An initial design of hohlraum driven by a shaped laser pulse. doi: 10.1017/S026303461000042X.
- LI, X., LAN, K., MENG, X., HE, X., LAI, D. & FENG, T. (2010). Study on Au + U + Au Sandwich Hohlraum wall for ignition targets. doi: 10.1017/S0263034609990590.
- LINDL, J.D., AMENDT, P., BERGER, R.L., GLENDINNING, S.G., GLENZER, S.H., HAAN, S.W., KAUFFMAN, R.L., LANDEN, O.L. & SUTER, L.J. (2004). The physics basis for ignition using indirect-drive targets on the National Ignition Facility. *Phys. Plasmas* **11**, 339–491.
- MCDONALD, J.W., SUTER, L.J., LANDEN, O.L., FOSTER, J.M., CELESTE, J.R., HOLDER, J.P., DEWALD, E.L., SCHNEIDER, M.B., HINKEL, D.E., KAUFFMAN, R.L., ATHERTON, L.J., BONANNO, R.E., DIXIT, S.N., EDER, D.C., HAYNAM, C.A., KALANTAR, D.H., KONIGES, A.E., LEE, F.D., MACGOWAN, B.J., MANES, K.R., MUNRO, D.H., MURRAY, J.R., SHAW, M.J., STEVENSON, R.M., PARHAM, T.G., VAN WONTERGHEM, B.M., WALLACE, R.J., WEGNER, P.J., WHITMAN, P.K., YOUNG, B.K., HAMMEL, B.A. & MOSES, E.I. (2006). Hard X-ray and hot electron environment in vacuum hohlraums at the National Ignition Facility. doi: 10.1063/1.2186927.
- PHILIPPE, F., CASNER, A., CAILLAUD, T., LANDOAS, O., MONTEIL, M.C., LIBERATORE, S., PARK, H.S., AMENDT, P., ROBEY, H. & SORCE, C.

- (2010). Experimental Demonstration of X-ray Drive Enhancement with Rugby-Shaped Hohlräume. *Phys. Rev. Lett.* **104**, 035004.
- ROBEY, H.F., AMENDT, P., PARK, H.-S., TOWN, R.P.J., MILOVICH, J.L., DÖPPNER, T., HINKEL, D.E., WALLACE, R., SORCE, C., STROZZI, D.J., PHILLIPPE, F., CASNER, A., CAILLAUD, T., LANDOAS, O., LIBERATORE, S., MONTEIL, M.-C., SÉGUIN, F., ROSENBERG, M., LI, C.K., PETRASSO, R., GLEBOV, V., STOECKL, C., NIKROO, A. & GIRALDEZ, E. (2010). High performance capsule implosions on the OMEGA laser facility with rugby hohlraums. *Phys. Plasmas* **17**, 056313.
- ROSEN, M.D., SCOTT, H.A., HINKEL, D.E., WILLIAMS, E.A., CALLAHAN, D.A., TOWN, R.P.J., DIVOL, L., MICHEL, P.A., KRUEER, W.L., SUTER, L.J., LONDON, R.A., HARTE, J.A. & ZIMMERMAN, G.B. (2011). The role of a detailed configuration accounting (DCA) atomic physics package in explaining the energy balance in ignition-scale hohlraums. *Hi. Ener. Density Phys.* **7**, 180.
- SCHNEIDER, M.B., HINKEL, D.E., LANDEN, O.L., FROULA, D.H., HEETER, R.F., LANGDON, A.B., MAY, M.J., MCDONALD, J., ROSS, J.S., SINGH, M.S., SUTER, L.J., WIDMANN, K. & YOUNG, B.K. (2006). Plasma filling in reduced-scale hohlraums irradiated with multiple beam cones. doi: 10.1063/1.2370697.
- SIGEL, R., PAKULA, R., SAKABE, S. & TSAKIRIS, G.D. (1988). X-ray generation in a cavity heated by 1.3 or 0.44 mm laser light III Comparison of the experimental results with theoretical predictions for X-ray confinement. *Phys. Rev. A* **38**, 5779.
- SUTER, L.J. (1985). Cross talk between modes in cylindrical hohlraums. Laser Program Annual Report 1985, Lawrence Livermore National Laboratory, Livermore, CA, UCRL-50055-85, pp. 30–31.
- VANDENBOOMGAERDE, M., BASTIAN, J., CASNER, A., GALMICHE, D., JADAUD, J.-P., LAFFITE, S., LIBERATORE, S., MALINIE, G. & PHILIPPE, F. (2007). Prolate-spheroid (“rugby-shaped”) hohlraum for inertial confinement fusion. doi: 10.1103/PhysRevLett.99.065004.